MOLECULAR AND CELLULAR BIOLOGY, Oct. 2011, p. 3988–3996 Vol. 31, No. 19
0270-7306/11/$12.00 doi:10.1128/MCB.05673-11

The LYR Protein Mzm1 Functions in the Insertion of the Rieske Fe/S Protein in Yeast Mitochondria▽

Aaron Atkinson,† Pamela Smith,† Jennifer L. Fox, Tie-Zhong Cui, Oleh Khalimonchuk, and Dennis R. Winge*

University of Utah Health Sciences Center, Departments of Medicine and Biochemistry, Salt Lake City, Utah 84132

Received 20 May 2011/Returned for modification 12 June 2011/Accepted 19 July 2011

The assembly of the cytochrome bc_1 complex in *Saccharomyces cerevisiae* is shown to be conditionally dependent on a novel factor, Mzm1. Cells lacking Mzm1 exhibit a modest bc_1 defect at 30°C, but the defect is exacerbated at elevated temperatures. Formation of bc_1 is stalled in *mzm1*Δ cells at a late assembly intermediate lacking the Rieske iron-sulfur protein Rip1. Rip1 levels are markedly attenuated in *mzm1*Δ cells at elevated temperatures. Respiratory growth can be restored in the mutant cells by the overexpression of the Rip1 subunit. Elevated levels of Mzm1 enhance the stabilization of Rip1 through physical interaction, suggesting that Mzm1 may be an important Rip1 chaperone especially under heat stress. Mzm1 may function primarily to stabilize Rip1 prior to inner membrane (IM) insertion or alternatively to aid in the presentation of Rip1 to the inner membrane translocation complex for extrusion of the folded domain containing the iron-sulfur center.

The ubiquinol-cytochrome *c* reductase (bc_1 complex, complex III) is a key component of the mitochondrial OXPHOS respiratory chain linking ubiquinol oxidation to cytochrome *c* reduction for terminal oxidation by cytochrome oxidase (C*c*O, complex IV). The eukaryotic bc_1 complex contains three redox subunits involved in electron transfer and 7 or 8 supernumerary subunits (18, 35). In contrast, the bacterial complex contains the core redox subunits and a single supernumerary subunit, if any (8). Of the core redox subunits, only the cytochrome *b* (Cob) subunit is encoded by the mitochondrial genome, whereas the other subunits are nuclear DNA encoded and imported into mitochondria from the cytoplasm. The Cob subunit anchors the core of the bc_1 complex that exists as a homodimeric unit within the inner mitochondrial membrane. The interface within the homodimeric unit consists of interactions of the Cob subunits and the matrix-facing Cor2 subunit (18, 35). In addition, the Rieske Fe/S protein Rip1 is intertwined between adjacent monomers with its globular domain in one unit and its transmembrane helix in the adjacent unit. The bc_1 complex is organized into higher-order supercomplexes, associating with C*c*O in *Saccharomyces cerevisiae* and both C*c*O and the complex I NADH oxidase in metazoans (30, 31). The bc_1 subunit Qcr9 is important for formation of this supercomplex and is likely to reside at the interaction interface (16).

The biogenesis of the bc_1 complex occurs as a modular assembly pathway with the mitochondrially encoded Cob seeding the complex assembly (37, 38). The nucleation by cytochrome *b* may explain why it is mitochondrially encoded in all known eukaryotes. An early core assembly complex containing Cob associated with two nucleus-encoded subunits, Qcr7 and Qcr8, is documented in yeast (Fig. 1) (3, 38). A second subassembly intermediate consists of the early core complex along with Cyt1, Cor1, Cor2, and Qcr6 (3, 37), lacking only Qcr9, Qcr10, and Rip1. This second intermediate of ~500 kDa, herein referred to as the late core intermediate, stably accumulates in yeast lacking either Rip1 or Qcr9. Since Rip1 contains the essential Fe/S center that facilitates electron transfer to the cytochrome c_1 subunit Cyt1, the assembly intermediate is devoid of function. Qcr10 is a late addition with Rip1 (5, 37) and appears to stabilize the complex, as Rip1 is labile within the bc_1 complex in the absence of Qcr10 (2). Consistent with its late addition, Rip1 can be extracted from the purified complex and reconstituted back to restore function (7).

The late core intermediate containing Cyt1 is likely a dimeric complex, but it fails to associate with C*c*O (4, 37). While the predicted mass for a dimeric complex lacking Qcr9, Qcr10, and Rip1 would be 400 kDa, the size of the second assembly intermediate is approximately 500 kDa. An additional molecule associated with the late core intermediate is the assembly factor Bcs1 (5). Bcs1 is an AAA ATPase that is critical for the biogenesis of the bc_1 complex. In the absence of Bcs1, yeast accumulates the late core intermediate and steady-state levels of Rip1 are diminished. Bcs1 was proposed to be an ATP-dependent chaperone that maintains the assembly intermediate in a competent state for subsequent insertion of Rip1 and Qcr10 (5).

A series of other assembly factors in addition to Bcs1 participate in biogenesis of the bc_1 complex in yeast (Fig. 1). Cbp3, Cbp4, and Cbp6 function at an early step in Cob translation and in addition associate with the newly synthesized Cob polypeptide (14, 19). Cyt2 is the CC1HL heme lyase that covalently attaches heme to apo-Cyt1 within the intermembrane space (IMS) (39, 40). Recently, Bca1 was shown to function in bc_1 assembly in fungi (22). Bca1 is postulated to act at an undefined step prior to insertion of Rip1 (22). A novel metazoan bc_1

* Corresponding author. Mailing address: University of Utah Health Sciences Center, Departments of Medicine and Biochemistry, Salt Lake City, UT 84132. Phone: (801) 585-5103. Fax: (801) 585-3432. E-mail: dennis.winge@hsc.utah.edu.
† These authors contributed equally to this work.
▽ Published ahead of print on 1 August 2011.

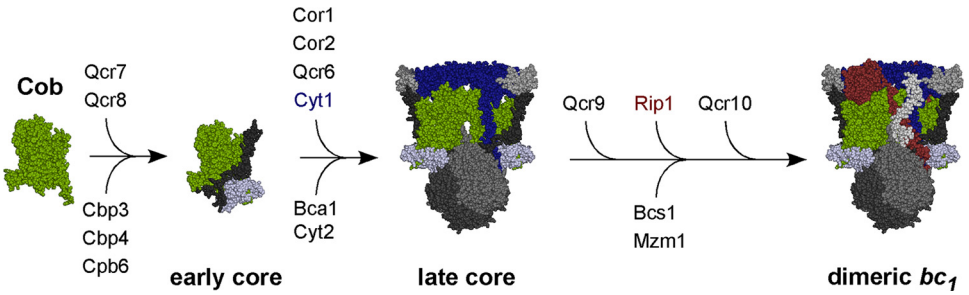

FIG. 1. Schematic for assembly of the bc_1 complex in yeast mitochondria. The Cob translational activator Cbp6 and assembly factor Cbp3 associate with the nascent polypeptide as it exits the mitochondrial ribosome. Cbp3 and Cbp6 remain bound to the newly synthesized Cob, and Cbp4 is recruited to this complex. The supernumerary subunits Qcr7 and Qcr8 associate with Cob (green) to form the early core complex. The core protein subunits, Cor1 and Cor2, along with Qcr6 subunits and the catalytic subunits of Cyt1 (blue), are added to form the late core complex. Bca1 is a recently identified assembly factor for bc_1 that acts prior to formation of the late core, and Cyt2 is the heme lyase. The assembly factors Bcs1 and Mzm1 assist in formation of the functional homodimeric bc_1 complex by assisting in the insertion of Rip1 (shown in ruby). Qcr9 and Qcr10 subunits are also added at a late step. Protein subunits of the bc_1 enzyme complex are listed above the arrows; nonsubunit proteins are listed below.

assembly factor, TTC19, was also recently reported (9). Patients with mutations in TTC19 show a marked bc_1 deficiency, with assembly intermediates being devoid of Rip1.

We identified a mitochondrial protein, Mzm1 (mitochondrial zinc maintenance), that when depleted in yeast results in a diminution in a mitochondrial labile, cationic zinc pool (1). In addition to the reduced labile zinc pool, *mzm1*Δ cells exhibit a destabilized bc_1 complex without perturbation in cytochrome oxidase or ATP synthase. The defect in bc_1 biogenesis in *mzm1*Δ cells is especially marked at 37°C. We show presently that Mzm1 is a bc_1 assembly factor functioning at the late assembly step of Rip1 insertion into the late core assembly intermediate. Mzm1 cooperates with Bcs1 in the Rip1 insertion step.

MATERIALS AND METHODS

Yeast strains and vectors. Strains were BY4741 (*MAT***a** *his3*Δ*1 leu2*Δ*0 met15*Δ*0 ura3*Δ*0*). The Cor2::TAP strain was purchased from Open Biosystems. The Bcs1::Myc strain was constructed through insertion of a PCR cassette (32) to append a 3′ tag with 13 repeats of the Myc epitope (EQKLISEEDL) and the *HIS3*MX6 coding sequence for selection. To generate the *mzm1*Δ deletion in these tagged strains, *MZM1* was replaced with a *Candida albicans URA3* coding sequence. Strains were grown either in 1% dextrose rich medium (yeast peptone dextrose) or in 2% galactose synthetic complete medium lacking relevant amino acids to maintain plasmid selection. For growth assays on solid medium, synthetic complete medium was supplemented with either 2% glucose or glycerol-lactate and relevant amino acids. Cultures for growth tests were grown in 2% glucose synthetic complete medium overnight and then normalized to absorbance at 600 nm and applied to solid medium in 1:10 serial dilutions.

Plasmids containing *MZM1*, *RIP1*, and *BCS1* were constructed as follows. *MZM1* was 3′ tagged with Myc and six histidine repeats and placed under the control of the *MET25* promoter and the *CYC1* terminator on a pRS413 vector. This Mzm1-MycHis plasmid was created by cloning a 5′ BamHI-to-3′ SalI fragment created by PCR into a vector containing the *MET25* promoter and *CYC1* terminator (24). To make point mutations in this plasmid-borne *MZM1*, Tyr11 and Arg23 were replaced with alanine by overlap extension PCR utilizing primers encoding the relevant substitution together with vector-based primers. The final PCR product was cloned into a pRS413 vector containing the *MET25* promoter and *CYC1* terminator by *in vivo* ligation. To target the C-terminal portion of Mzm1 beginning at glutamate 27 to the mitochondrial matrix, the Sod2 mitochondrial targeting sequence corresponding to amino acids 1 to 26 was cloned into a pRS413 vector as an XbaI/BamHI fragment, and the *MZM1* sequence (from either the Mzm1-HisMyc clone or the point mutants) was appended following the BamHI site using overlapping oligonucleotides and *in vivo* gap repair. *RIP1* was cloned by PCR using primers anchored in the *RIP1* promoter and terminator appended with vector sequence to facilitate *in vivo* gap repair into BamHI- and NotI-digested pRS vector systems. This strategy created both pRS415 and pRS425 vectors bearing *RIP1* under the control of its endogenous promoter and terminator. Using these *RIP1* plasmids as a template, a plasmid containing the S183C point mutation in *RIP1* was generated by overlap extension PCR utilizing primers encoding the substitution together with vector-based primers. *BCS1* was 3′ tagged with Myc and cloned into either pRS416 or pRS426 vector under the control of the *MET25* promoter and the *CYC1* terminator (24). The tag was added by PCR, using primers appended with vector sequence to facilitate *in vivo* gap repair of the PCR product into the vectors digested with either 5′ BamHI/3′ PstI (pRS416) or 5′ EcoRI/3′ XhoI (pRS426). All vectors were confirmed by sequencing.

Suppression of *mzm1*Δ cells. The *mzm1*Δ strain was transformed with a YEp library derived from the *coa2*Δ strain (29). Approximately 52,000 transformants were recovered on glucose-containing synthetic complete medium lacking uracil. Colonies were then replica plated onto glycerol-lactate synthetic complete plates lacking uracil and grown at 37°C. Plasmids from recovered colonies were isolated and sequenced with vector-based primers.

Preparation of mitochondria. Mitochondria were isolated as described previously (6). Briefly, lyticase was used to create spheroplasts that were subsequently ruptured by vortexing with glass beads or Dounce homogenizing, and mitochondria were isolated by differential centrifugation. For some experiments, mitochondria were further purified using ultracentrifugation through a discontinuous Histodenz (Sigma-Aldrich) gradient (14% and 22%). The total mitochondrial protein concentration was estimated using the Bradford method.

Immunoblotting and BN-PAGE analysis. For SDS-PAGE, 10 to 30 μg of protein samples or mitochondria was separated on 12 or 15% polyacrylamide gels and transferred to nitrocellulose membranes. Membranes were blocked prior to detection using 5 to 10% nonfat dry milk in phosphate-buffered saline (PBS) with or without 0.01% Tween 20. Blue native PAGE (BN-PAGE) was performed essentially as described previously (34) with either 1% digitonin or 1% dodecylmaltoside. Either chemiluminescent reagents with horseradish peroxidase-conjugated secondary antibodies or infrared (IR) dye-conjugated secondary antibodies (Li-Cor) were used to visualize proteins. Antibodies either were purchased or were generous gifts: anti-Myc (Roche Diagnostics), anti-Sdh2 (21st Century Biochemicals), antiporin (Molecular Probes), anti-Cox2 (Mitosciences), anti-TAP (Open Biosystems), anti-Rip1 and anti-Cor1/Cor2 (B. Trumpower), anti-Cyt1 (B. Meunier), anti-Yah1 and anti-Aco1 (R. Lill), and anti-F_1 ATPase beta subunit Atp2 (A. Tzagoloff).

Depletion of Yah1. Strains were a kind gift from R. Lill and are described in reference 20. Gal-*YAH1* or wild-type (WT) cells were precultivated in galactose-containing minimal medium for 24 h at 30°C. Cells were washed and transferred to minimal medium containing 2% lactate and 0.1% glucose. Cells were diluted 20-fold into fresh lactate medium containing 0.1% glucose every 20 h. After 85 h, mitochondria from WT and Gal-*YAH1* cells were isolated as described above. Depletion of Yah1 was verified by immunoblotting.

Complex III purification. Mitochondria from both the Cor2::TAP and Cor2::TAP *mzm1*Δ strains (200 μg) were lysed in 450 μl of IPP150 buffer (10 mM Tris, pH 7.4, 150 mM $NaCl_2$, 1 mM phenylmethylsulfonyl fluoride [PMSF], with 1% digitonin) on ice for 10 min. Lysates were clarified by centrifugation at 10,000 × *g* for 10 min at 4°C. IgG magnetic beads (50 μl; NEB S1431S) were rinsed three times in IPP150 buffer (with 0.5% digitonin). Beads were added to each lysate and incubated overnight at 4°C with rotation. Beads were precipi-

tated magnetically and rinsed two times in tobacco etch virus (TEV) protease buffer (10 mM Tris, pH 7.4, 150 mM $NaCl_2$, 0.5 mM EDTA, 1 mM PMSF, 0.1 M dithiothreitol [DTT], and 0.5% digitonin). TEV protease (100 units; Invitrogen) was added to 1 ml TEV buffer, and 500 μl was added to beads and incubated for 1 h at room temperature. As the Cor2::TAP strain remained associated with the IgG beads after TEV treatment, IgG beads were precipitated and rinsed three times in 0.5 ml calmodulin binding buffer (10 mM Tris, pH 7.4, 150 mM $NaCl_2$, 4 mM $CaCl_2$, 1 mM magnesium acetate, 1 mM imidazole, 10 mM 2-mercaptoethanol, and 0.5% digitonin). Calmodulin beads (100 μl) were rinsed in 0.5 ml binding buffer three times, resuspended in an 0.5-ml final volume, and added directly to precipitated IgG beads. The mixed beads were incubated at 4°C with rotation for 4 h. IgG beads were removed from the calmodulin bead bed magnetically. Calmodulin beads were rinsed three times in 0.5 ml buffer, with precipitation between rinses with brief spins. Precipitated beads were boiled in 0.1 ml Laemmli buffer and loaded into duplicate lanes of Bis-Tris 12% NuPAGE gels (Invitrogen) and run in the manufacturer's recommended morpholineethanesulfonic acid (MES) SDS running buffer. Gels were divided for parallel immunoblot analysis and Sypro ruby staining (Invitrogen) as recommended by the manufacturer. For mass spectrometry, indicated Sypro ruby-stained bands were excised from the gel for liquid chromatography-tandem mass spectrometry (LC-MS/MS) analysis at the University of Utah Mass Spectrometry and Proteomics Core.

Immunoprecipitation of Mzm1. *mzm1*Δ cells expressing Sod2-Mzm1-MycHis and WT cells were grown on synthetic galactose medium with selection, and mitochondria were isolated as described above. Mitochondria (1 mg protein/ml) were lysed at 4°C in lysis buffer (20 mM Tris, pH 7.4, 150 mM NaCl, 1 mM PMSF, 1% digitonin, 0.1 mM EDTA, and 10% glycerol) and clarified by centrifugation at 20,000 × *g* for 15 min. Solubilized mitochondrial proteins were applied to Myc-agarose beads (20-μl settled volume) at 4°C and then washed with 60 column volumes of wash buffer (20 mM Tris, pH 7.4, 150 mM NaCl, 1 mM PMSF, 0.3% digitonin, 0.1 mM EDTA, and 10% glycerol). Bound proteins were eluted either by boiling or with 10% SDS.

Mitochondrial enzymatic activity assays. The bc_1 activity of isolated mitochondria was measured spectrophotometrically by supplying decylubiquinol and cytochrome *c* and following the rate of reduction of cytochrome *c* (while inhibiting C*c*O with 2 mM KCN). Decylubiquinol was prepared as described previously (1). The activity assay was performed with 30 μM decylubiquinol, 0.4 mg/ml cytochrome *c* (from horse heart; Sigma-Aldrich), and 10 to 30 μg total mitochondrial protein in 40 mM potassium phosphate, pH 6.8, with 0.5% Tween 80. The initial rate of cytochrome *c* reduction at 550 nm was measured by an Agilent 8453 spectrophotometer. Succinate dehydrogenase (SDH) activity of 15 μg of isolated mitochondria in potassium phosphate (pH 6.8) buffer with 0.5% Tween 80 (TMPD) was measured with 10 mM succinate, 90 μM decylubiquinol, and 80 μM dichlorophenolindophenol (DCPIP) (Sigma-Aldrich) spectrophotometrically at 600 nm. Aconitase activity of 15 μg of isolated mitochondria in TMPD was measured spectrophotometrically with *cis*-aconitate at 240 nm.

Metal analysis. Total metal levels were determined by inductively coupled plasma-optical emission spectroscopy (ICP-OES) as described previously (1). The zinc-specific fluorophore RhodZin-3 dipotassium salt (Molecular Probes) was used to assess labile zinc concentrations as described previously (1).

Absorbance spectroscopy of heme. For optical absorption spectra, 1.5 mg of purified mitochondria grown in galactose medium was solubilized in PBS buffer containing 1% dodecylmaltoside. Each spectrum represents the calculated difference spectrum of the reduced (dithionite) minus oxidized (ferricyanide) cytochromes and was recorded by an Agilent 8453 spectrophotometer. Absorption maxima at 550, 560, and 603 nm correspond to cytochromes *b*, *c*, and a,a_3, respectively.

RESULTS

Labile zinc pool in mitochondria is dependent on functional bc_1 complex. We reported previously that *mzm1*Δ cells have reduced mitochondrial zinc, especially in a labile matrix zinc pool accessible to the Zn(II)-chelating fluorophore Rhodzin-3 (1). The mutant cells are hypersensitive to further attenuation of this labile zinc pool. In addition, *mzm1*Δ cells are impaired in respiration with a specific defect in the bc_1 complex, especially at 37°C. We addressed the link between bc_1 complex function and mitochondrial labile zinc by quantifying zinc levels in yeast mutants impaired in bc_1 assembly. Qcr7 is an essential bc_1 complex subunit that stabilizes the first assembly intermediate containing cytochrome *b* (Fig. 1) (3, 38). In contrast, Qcr9 is one of the last subunits added during the assembly process and, much like Mzm1, is critical only for bc_1 function at 37°C (12, 28). Mitochondria isolated from yeast lacking either Qcr7 or Qcr9 were used for quantitation of total zinc by ICP-OES and of labile zinc with the RhodZin-3 fluorophore. The two mutants exhibit similar diminutions in labile zinc (data not shown). Likewise, the labile mitochondrial zinc pool was also attenuated in cells lacking the bc_1 assembly factor Bcs1. Thus, the zinc impairment in *mzm1*Δ cells likely arises from the deficiency of the bc_1 complex and not from a specific effect of Mzm1 on mitochondrial zinc.

Rip1 is deficient in *mzm1*Δ cells. We sought to deduce the basis for the defect in bc_1 function in *mzm1*Δ cells. Using a yeast strain with a chromosomal TAP purification tag on the Cor2 bc_1 subunit, we purified the complex from wild-type (WT) and *mzm1*Δ cells. After a two-step affinity purification, visualization of the final eluate by Sypro staining after SDS-PAGE revealed an array of bc_1 complex subunits (Fig. 2A). Mass spectrometry was used to validate the identity of several of the bands in the WT cells, including Cor1, Cor2, Rip1, Qcr8, and Qcr9. The sample recovered from *mzm1*Δ cells showed similar levels of most subunits, with the exception of Rip1. To confirm the attenuation in Rip1, immunoblotting was performed (Fig. 2A, IB). Rip1 was markedly low in *mzm1*Δ cells, despite equal loading of Cor2. Qcr9 and Qcr10 are normally added late in assembly along with Rip1 (37), but no obvious defect was observed in the level of Qcr9 in the complex isolated from *mzm1*Δ cells. Steady-state levels of Rip1 were attenuated in the mutant cells, especially at 37°C (Fig. 2B).

Previous studies on bc_1 biogenesis revealed that a stable assembly intermediate lacking Rip1 is apparent in cells lacking Bcs1 or Qcr9 (5). This late core assembly intermediate is visualized by BN-PAGE using antisera to subunits preceding Rip1 insertion. Digitonin extracts of mitochondria isolated from *mzm1*Δ cells separated on BN-PAGE show a bc_1 assembly of lower mass than the dimeric complex (Fig. 2C, III*). Since the bc_1 assembly intermediate is deficient in Rip1, the lower-mass complex is not apparent using antisera to Rip1. The bc_1 intermediate as purified above contains the mitochondrion-encoded Cob subunit and its two cytochrome *b* moieties. The presence of hemylated Cob was shown by difference spectroscopy of membranes from *mzm1*Δ cells (Fig. 2D). Heme *b* levels were not markedly attenuated in *mzm1*Δ cells relative to WT. This result is consistent with the previous observation that heme insertion into Cob occurs upon formation of the early core assembly intermediate (27).

Since residual bc_1 activity exists in *mzm1*Δ cells, we attempted a suppressor screen of *mzm1*Δ cells to isolate extragenic suppressors. The mutant cells exhibit a marked growth defect at 37°C on glycerol-lactate medium (Fig. 3A, "vec"). Although no spontaneous suppressor mutants were recovered, respiration-competent clones were obtained after transformation of *mzm1*Δ cells with a high-copy-number yeast DNA library. Transformants were screened by replica plating at 30 and 37°C. In addition to the expected *MZM1* clones, we recovered two clones with inserts spanning the *RIP1* locus (Fig. 3A, S1). The respiratory growth of the clones was abrogated by pregrowth in 5-fluoroorotic acid used to shed the vector. Two

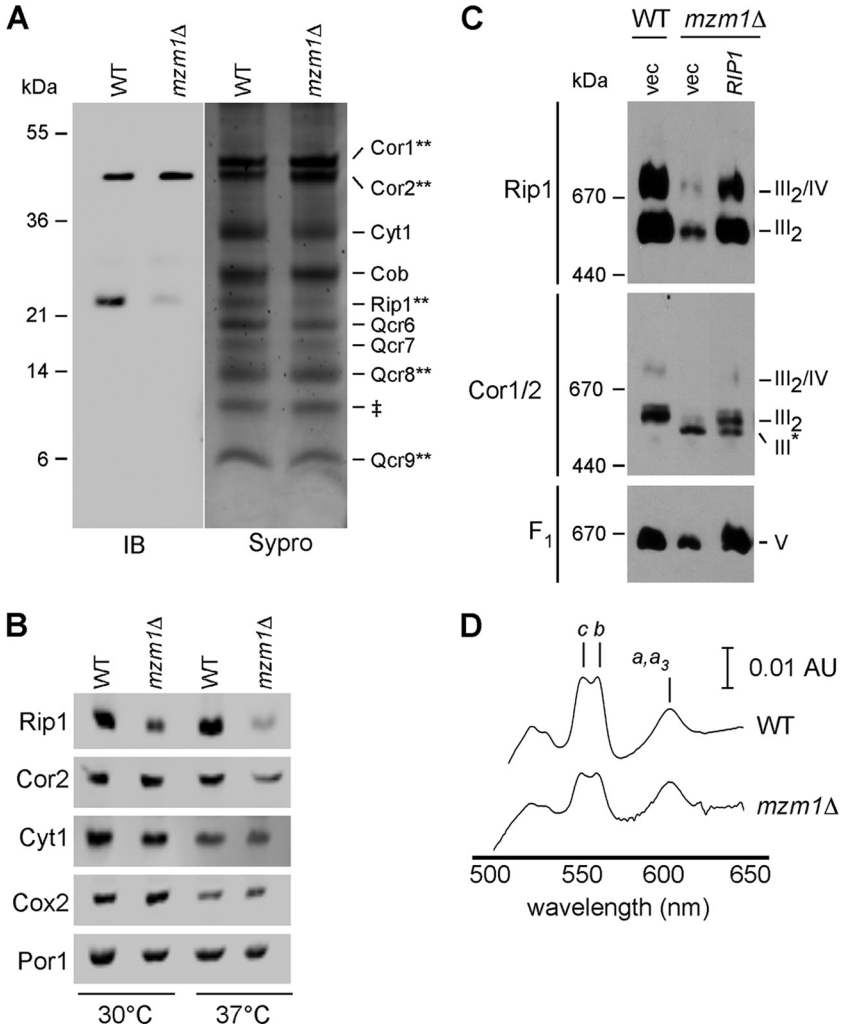

FIG. 2. Characterization of bc_1 complex components and supercomplex formation in *mzm1*Δ cells. (A) bc_1 complex purification via tandem affinity purification of Cor2::TAP in strains with and without Mzm1 from mitochondria solubilized by 1% digitonin. SDS-PAGE gels of the purification products were stained with Sypro ruby, and the bands were identified by mass spectrometry (where indicated by **) along with immunoblotting (IB) to identify Cor2 (anti-TAP) and Rip1 (anti-Rip1). ‡, a band with a mass similar to that of Qcr10 was observed by Sypro staining; we failed to confirm its identity as Qcr10. (B) SDS-PAGE immunoblot of mitochondria isolated from cultures grown at 30 and 37°C. (C) BN-PAGE immunoblot of mitochondria solubilized by 1% digitonin. The late core subassembly intermediate is designated by III*. (D) Optical absorbance spectra were recorded of reduced minus oxidized cytochromes in WT and *mzm1*Δ mitochondrial detergent lysates. AU, absorbance unit.

new vectors were engineered containing the *RIP1* locus as low-copy-number (YCp) and high-copy-number (YEp) plasmids. Transformation of *mzm1*Δ cells with these vectors revealed that 37°C respiratory growth was restored in the mutant cells with either *RIP1*-containing vector (Fig. 3B). The overexpression of *RIP1* restored steady-state Rip1 levels in *mzm1*Δ cells (Fig. 3C), along with restoring the intact bc_1 complex visualized by BN-PAGE after dodecylmaltoside solubilization of mitochondria (Fig. 3D). Immunoblotting for the F_1/F_o ATP synthase (complex V) was used to show equivalent protein loads per lane. BN-PAGE with digitonin solubilization revealed the restoration of C*c*O/bc_1 supercomplexes upon *RIP1* overexpression (Fig. 3E). Consistent with the BN-PAGE results, elevated levels of Rip1 increased bc_1 enzymatic activity to approximately 60% of WT levels (Fig. 3F).

As evidenced above, cells lacking Mzm1 have impaired bc_1 activity due to attenuated levels of Rip1 insertion, similar to the phenotype reported for *bcs1*Δ cells (5). To assess the relationship between Mzm1 and Bcs1, we tested whether overexpression of *BCS1* would restore respiratory growth to *mzm1*Δ cells (Fig. 3B). Overexpression of *BCS1* gave only a modest improvement in glycerol-lactate growth and bc_1 activity of the mutant cells, which was clearly not to the same extent as overexpression of *RIP1* (Fig. 3B and F). Bcs1 steady-state protein levels are not attenuated in *mzm1*Δ cells, unlike Rip1 levels (Fig. 3G). Thus, the defect in *mzm1*Δ cells correlates with impaired Rip1 insertion into the bc_1 complex.

Late step in Rip1 maturation is impaired in *mzm1*Δ cells. The maturation of Rip1 into the bc_1 complex involves a series of steps. Rip1 is synthesized in the cytoplasm with an N-terminal mitochondrial targeting sequence that is proteolytically cleaved by the matrix processing protease (MPP) during im-

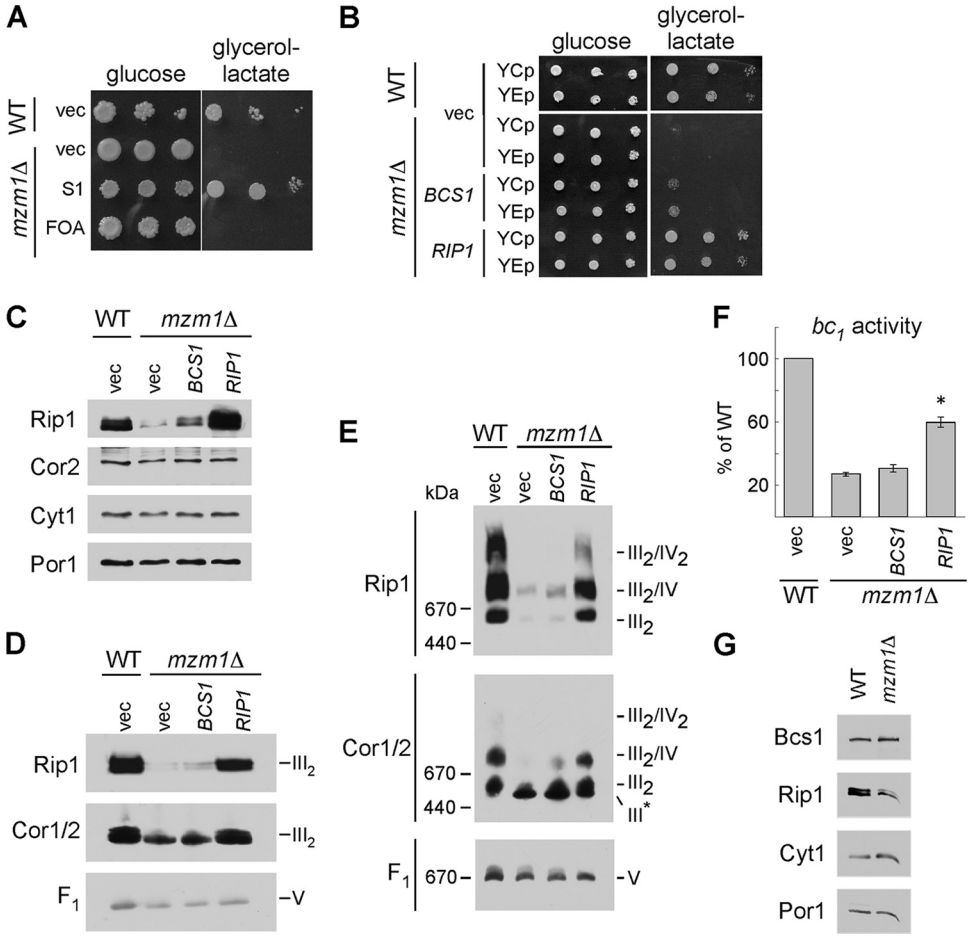

FIG. 3. Suppression of the 37°C growth defect and rescue of the reduced Rip1 levels, supercomplex formation, and bc_1 complex activity of *mzm1*Δ. (A) Growth test at 37°C on glucose or glycerol-lactate medium of *mzm1*Δ cells transformed with vector control (vec) or a plasmid isolated from the suppression screen (S1), which was identified by sequencing to contain *RIP1*. Loss of this *RIP1*-containing plasmid was induced by 5-fluoroorotic acid treatment (FOA). (B) Growth test at 37°C on glucose or glycerol-lactate medium of *mzm1*Δ cells transformed with low-copy-number (YCp) and high-copy-number (YEp) vector control or plasmids containing *BCS1* or *RIP1*. (C to E) SDS-PAGE (C) and BN-PAGE immunoblots with either 1% dodecylmaltoside solubilization (D) or 1% digitonin solubilization (E) of mitochondria from *mzm1*Δ cells transformed with YEp vector control or plasmids containing *BCS1* or *RIP1*. The late core subassembly intermediate is designated by III*. (F) bc_1 complex activity of mitochondria from *mzm1*Δ cells transformed with high-copy-number vector control or plasmids containing *BCS1* or *RIP1*, shown as a percentage of WT activity, with the asterisk indicating significantly increased activity relative to *mzm1*Δ with vector control ($n = 6 \pm$ standard deviation). Statistical significance was determined by analysis of variance with Bonferroni's *post hoc* test in Kaleidagraph. (G) SDS-PAGE immunoblot of mitochondria from Bcs1::Myc cultures with and without Mzm1. Bcs1 protein levels were identified using anti-Myc antibody.

port through the TIM23 complex (15). The protein is fully translocated into the matrix compartment for subsequent insertion into the inner membrane (IM). In yeast, a second proteolytic cleavage by Oct1 removes an additional 8 residues. The remaining steps in Rip1 maturation involve insertion of the 2Fe-2S cluster within the matrix, translocation of the Fe/S domain across the IM, and finally the formation of a disulfide bond (11, 23, 25, 26). Processing of the residual Rip1 by MPP and Oct1 appears normal in *mzm1*Δ cells (Fig. 4A). No precursor polypeptide consistent with impaired MPP cleavage was evident in *mzm1*Δ cells, although incomplete cleavage of the intermediate precursor was apparent in both WT and mutant cells. This cleavage of the intermediate Rip1 precursor by Oct1 is not required for Rip1 insertion into the bc_1 complex (26).

The Rip1 defect in *mzm1*Δ cells is unlikely to be due to impaired Fe/S cluster formation based on previous studies. Neither formation of the Fe/S center nor the disulfide bond was found to be important for the IM insertion of Rip1 (13, 23). To confirm this observation on the formation of the Fe/S cluster, we repressed the expression of the essential mitochondrial matrix ferredoxin, Yah1, required for Fe/S cluster biogenesis using a *GAL10-YAH1* strain (20). Propagation of these cells on lactate-containing medium results in the repression of *YAH1* expression, resulting in an impairment in Fe/S cluster biogenesis within the mitochondrial matrix (21). Depletion of Yah1 results in a marked attenuation in the activity of mitochondrial Fe/S cluster proteins aconitase, succinate dehydrogenase, and bc_1 (Fig. 4B), as was shown previously (20). Whereas steady-state levels of Sdh2 (Fig. 4C) and the SDH complex on BN-PAGE (Fig. 4D) were markedly attenuated, Rip1 levels were not significantly perturbed and Rip1 was associated with the bc_1 complex by BN-PAGE (Fig. 4C and D).

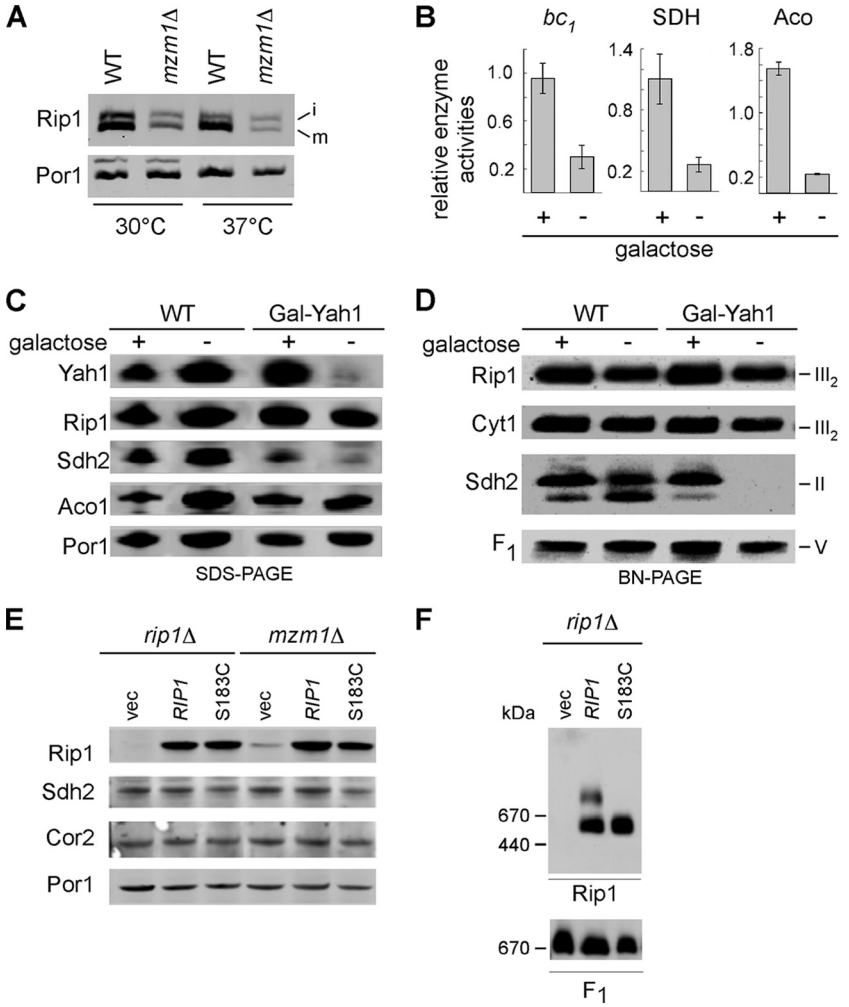

FIG. 4. Rip1 processing and Fe/S cluster insertion are not impaired in *mzm1*Δ cells. (A) SDS-PAGE immunoblot of mitochondria isolated from WT and *mzm1*Δ cultures grown at 30 and 37°C. Intermediate (i) and mature (m) forms of Rip1 are indicated. (B) Analysis of cytochrome *c* reductase (bc_1), succinate dehydrogenase (SDH), and aconitase (Aco) activities of mitochondria from WT or Gal-*YAH1* cells grown in either galactose-replete (+) or -deficient (−) medium, where the depletion of Yah1 by lactate replacement of galactose results in a lack of Fe/S cluster biogenesis. The results are presented relative to the activities measured for the mitochondrial enzymes of either WT or Gal-*YAH1* cells grown in the presence of galactose (+). Error bars indicate standard deviations; $n = 3$. (C and D) SDS-PAGE (C) and BN-PAGE (D) with 1% dodecylmaltoside solubilization of mitochondria from WT or Gal-*YAH1* cells grown in either galactose or lactate-replete medium. (E) SDS-PAGE and immunoblotting of mitochondria from *rip1*Δ or *mzm1*Δ cells transformed with high-copy-number vector control or plasmids containing WT or S183C Rip1. (F) BN-PAGE with 1% digitonin solubilization of mitochondria isolated from *rip1*Δ cells expressing either WT or S183C Rip1 (mutant lacking a Fe/S cluster).

Likewise, the S183C Rip1 mutant that was reported to lack a Fe/S cluster is stably expressed in both *mzm1*Δ and *rip1*Δ cells (Fig. 4E) and is inserted into the bc_1 complex (Fig. 4F). These studies confirm the previous observations showing that Fe/S cluster insertion is not a prerequisite for Rip1 IM insertion (5, 13). Thus, the impaired insertion of Rip1 into the bc_1 complex in *mzm1*Δ cells is not a result of a failure to insert Fe/S into Rip1. The remaining step in Rip1 maturation is its insertion in the IM with the globular domain containing the Fe/S cluster facing the IMS side of the membrane.

Rip1 is stabilized by Mzm1. As mentioned, *mzm1*Δ cells exhibit attenuated levels of Rip1. To assess whether Mzm1 contributes to the stabilization of Rip1 prior to membrane insertion, we took advantage of the low, albeit unincorporated, levels of Rip1 in *bcs1*Δ cells (27). Overexpression of Mzm1 in *bcs1*Δ cells gave variable results on Rip1 stabilization, but coexpression of Rip1 and Mzm1 gave a highly reproducible stabilization of Rip1 levels compared to expression of Rip1 alone in *bcs1*Δ cells (Fig. 5A). The Mzm1-mediated stabilization of Rip1 was apparent in cells isolated at both 30 and 37°C. The observed stabilization of Rip1 by Mzm1 suggested that the two proteins may transiently interact. Immunoprecipitation of a Myc-tagged Mzm1 allele in WT cells with anti-Myc antibody-conjugated beads resulted in the coprecipitation of Rip1 (Fig. 5B). No Rip1 was precipitated in WT cells lacking a Myc-tagged Mzm1 allele.

The LYR motif of Mzm1 is important for its function. Mzm1 is a 14-kDa polypeptide that contains only one conserved motif, a poorly defined variant of the LYR motif that is seen in Isd11 and Sdh6 (10, 33) (Fig. 6A). To address whether the

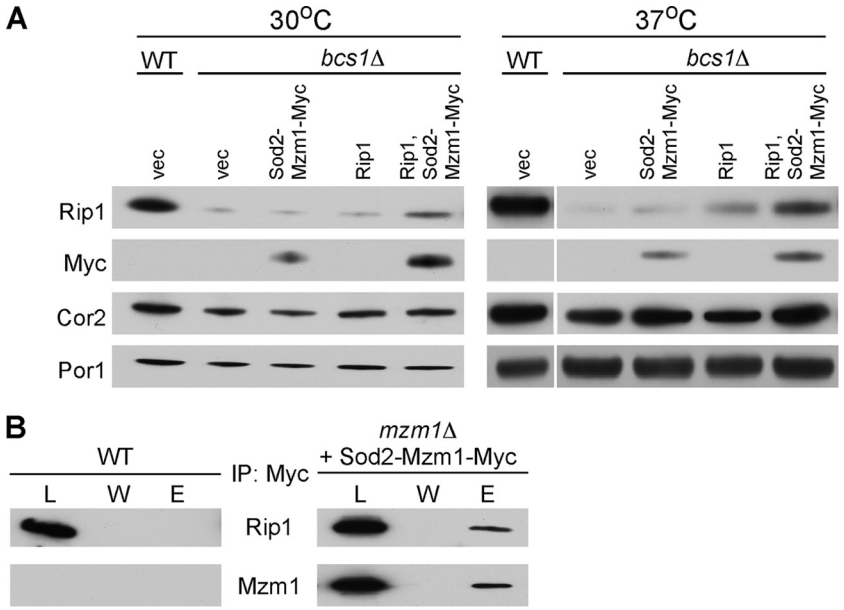

FIG. 5. Mzm1 stabilizes and interacts with Rip1. (A) SDS-PAGE immunoblot of mitochondria from WT and *bcs1*Δ cells cultured at either 30 or 37°C expressing indicated plasmids. Mzm1 levels were identified with anti-Myc antibody. (B) Immunoprecipitation of WT or *mzm1*Δ cells overexpressing Sod2-Mzm1-Myc with anti-Myc-agarose beads. Three percent of the total extracts (L), the entire fraction of the last wash (W), and 20% of the bead eluate (E) were analyzed by SDS-PAGE and immunoblotting with anti-Rip1 or anti-Myc (Mzm1) antibodies.

LYR motif is functionally important, a Tyr11Ala (Y11A) mutant was generated for *in vivo* testing. The mutations were introduced in the gene expressed from its own promoter as well as full- and partial-length fusion genes containing the *MET25* promoter and Sod2 mitochondrial target sequence (MTS).

The LYR motif in Mzm1 occurs in the N-terminal segment of the protein that is predicted by the MitoProt II algorithm to be a cleaved mitochondrial target sequence consisting of 26 residues. Removal of the candidate MTS from Mzm1 abolished function (data not shown). Growth of *mzm1*Δ cells at 37°C was supported by fusion of the Sod2 MTS to full-length Mzm1; however, Sod2 MTS fused to residues 27 to 124 of Mzm1 failed to support respiratory growth in *mzm1*Δ cells at 37°C (Fig. 6B). Lastly, in either the native or the Sod2-Mzm1 fusion protein, replacement of Tyr11 in the LYR motif with alanine (Y11A) failed to support growth on glycerol-lactate (Fig. 6B and data not shown).

To assess whether Mzm1 is processed by the MPP protease, we utilized the Sod2 fusion proteins together with mutating the candidate Arg (Arg23) that may serve as the MPP protease docking site to an alanine (R23A). Mitochondria isolated from *mzm1*Δ cells harboring either WT, R23A, or Sod2-Mzm1 fusions were used for steady-state PAGE protein analysis (Fig. 6C). The size of the Mzm1 polypeptide was equivalent in comparing the WT Mzm1 protein to either R23A or the Sod2 fusion with full-length Mzm1. However, the Sod2 MTS fusion with the truncated Mzm1 lacking its putative MTS exhibited a markedly smaller polypeptide. These results show that Mzm1 lacks a cleavable MTS and that Tyr11 within the LYR motif of the mature protein is functionally important.

DISCUSSION

Mzm1 is presently shown to be an assembly factor for the bc_1 complex in yeast. The conservation of Mzm1 in metazoans suggests that it may have a conserved role in higher eukaryotes. Mzm1 functions at a late step in bc_1 complex assembly during the insertion of the Rip1 Rieske Fe/S protein. Cells lacking Mzm1 exhibit a modest bc_1 defect at 30°C, but the defect is exacerbated at elevated temperatures. Rip1 levels are markedly attenuated at elevated temperatures in *mzm1*Δ cells. Previously, we demonstrated that cells lacking Mzm1 are compromised in a mitochondrial zinc pool accessible to the zinc-responsive RhodZin-3 fluorophore (1). Further attenuation in the mitochondrial zinc pool by targeting a heterologous Zn-binding protein to the mitochondrial matrix leads to a respiratory deficiency. We show presently that the mitochondrial zinc deficiency is not a unique phenotype of *mzm1*Δ cells. Rather, cells lacking the bc_1 complex show the same attenuated labile zinc pool. Yeasts lacking either of two structural subunits of the bc_1 complex, Qcr7 and Qcr9, or lacking an essential bc_1 assembly factor Bcs1 are compromised in the zinc pool. The basis for the attenuation in labile matrix zinc in bc_1-deficient cells as well as cells deficient in the citric acid cycle enzymes Cit1 and Mdh1 shown previously (1) remains unclear.

The biogenesis of the bc_1 complex occurs in a modular assembly pathway (3, 36, 38) (Fig. 1). The early central core complex consisting of Cob, Qcr7, and Qcr8 is evident in cells stalled at downstream assembly steps (38). The early core complex is converted to the late core subassembly intermediate with the addition of Cyt1, Cor1, Cor2, and Qcr6 subunits and occasionally Qcr9 (3, 37). This late core intermediate lacks

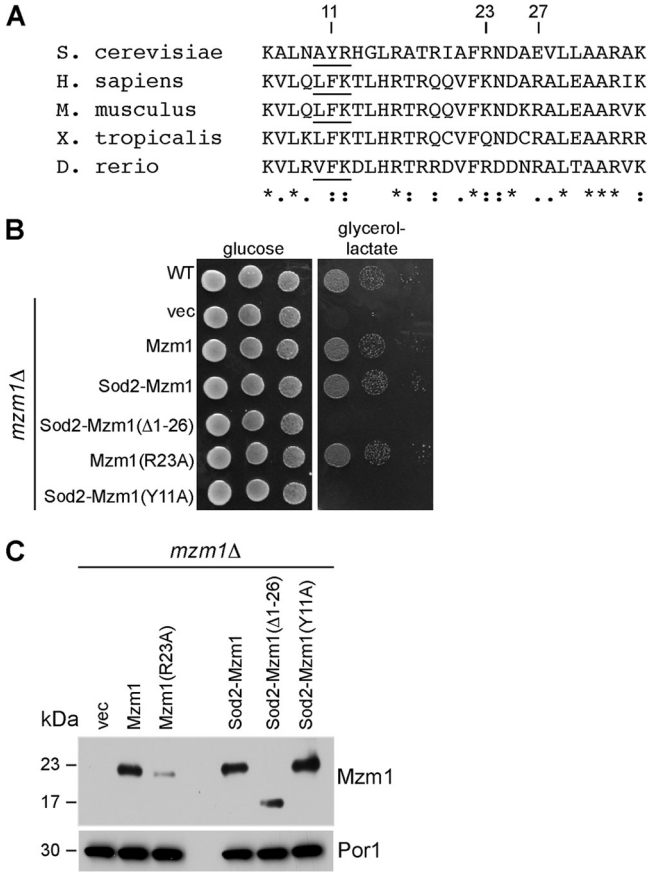

FIG. 6. The LYR motif of Mzm1 is important for its function. (A) Mzm1 protein sequences are shown with conserved segments in the N-terminal region. The Tyr in the LYR (AYR) motif is residue 11. *H. sapiens*, *Homo sapiens*; *M. musculus*, *Mus musculus*; *X. tropicalis*, *Xenopus tropicalis*; *D. rerio*, *Danio rerio*. (B) WT cells and *mzm1*Δ cells expressing vector, high-copy-number Mzm1, low-copy-number Sod2-Mzm1, low-copy-number Sod2-Mzm1 (Δ1–26), high-copy-number Mzm1 (R23A), and low-copy-number Sod2-Mzm1 (Y11A) were grown in synthetic selective medium, serially diluted, and spotted on yeast extract-peptone medium containing glucose or glycerol-lactate carbon sources. Cells were incubated at 37°C. (C) Mitochondria from the respective strains in panel B were analyzed by SDS-PAGE and immunoblotted with anti-Myc antibody to visualize Mzm1.

only Qcr10 and Rip1 (5, 37). Cob and Cyt1 contain their heme *b* and heme *c* cofactors, respectively (3, 37). This late core complex is of greater stability than the early core complex and can be isolated after solubilization in either digitonin or Triton X-100. An unresolved issue concerns the step of bc_1 dimerization (37). The late core intermediate is either a dimeric unit with an associated Bcs1 assembly factor or a monomeric unit with additional assembly subunits such as an oligomerized Bcs1. However, since the dimer interface consists mainly of cytochrome *b* helices, dimerization is believed to occur early in the assembly pathway (37, 38).

Cells lacking Mzm1 are stalled at the late core assembly intermediate, which in this case contains Qcr9. Respiratory growth at 37°C can be restored in the *mzm1*Δ cells by the overexpression of the Rip1 subunit. The attenuated level of Rip1 in *mzm1*Δ cells is consistent with a role of Mzm1 in Rip1 maturation.

Rip1 maturation has previously been shown to involve the complete import of Rip1 into the matrix, without a stop transfer within the IM. In support of a complete import of Rip1 into the mitochondrial matrix, expression of Rip1 from the mitochondrial genome is able to complement a *rip1*Δ strain, suggesting that Rip1 maturation occurs within the matrix (26). In yeast, two proteolytic processing steps occur, one being the removal of the mitochondrial target sequence by MPP and the second the removal of an octapeptide sequence by Oct1. The 2Fe-2S center is likely formed in Rip1 within the matrix by the resident iron-sulfur cluster (ISC) Fe/S cluster system. Subsequent to Fe/S cluster formation, membrane insertion of Rip1 occurs along with the extrusion of the C-terminal Fe/S domain to the IMS side of the IM. An important disulfide bond forms in the Fe/S domain, and this may occur after extrusion of the folded domain to the IMS side of the IM. The redox potential of the IMS is more oxidizing than the matrix or cytoplasm, and numerous proteins within this space contain disulfides (17).

The block in Rip1 insertion into the bc_1 complex in *mzm1*Δ cells likely occurs at a later step in Rip1 maturation, as evidenced by the lack of impairment in either MPP or Oct1 processing in *mzm1*Δ cells. Although the mutant cells have somewhat higher levels of the i-Rip1 species without the Oct1 cleavage, the Oct1 processing step is not essential for IM insertion or catalytic activity (26). Formation of the Fe/S center is not a prerequisite for IM insertion of Rip1, so that step is not likely impaired in *mzm1*Δ cells. IM insertion and extrusion of the Fe/S domain are steps that may be impaired in the mutant cells. However, Mzm1 is not essential to these steps since limited bc_1 activity is apparent at 30°C and a modest increase in Rip1 expression can suppress the respiratory defect in *mzm1*Δ cells. One revealing defect in *mzm1*Δ cells is the impaired stabilization of Rip1 prior to IM insertion. Rip1 levels are markedly attenuated at elevated temperatures in *mzm1*Δ cells. Rip1 is also destabilized in *bcs1*Δ cells in which Rip1 IM insertion is likely blocked. In the absence of IM insertion, Rip1 has limited stability, especially at elevated temperatures. Under these conditions, Mzm1 has a greater role in Rip1 maturation. Elevated levels of Mzm1 enhance the stabilization of Rip1, suggesting that Mzm1 may be an important Rip1 chaperone under cell stress.

Mzm1 may function primarily as a Rip1 chaperone to stabilize Rip1 prior to IM insertion or, alternatively, as a chaperone that aids in the presentation of Rip1 to the maturing bc_1 complex. This maturation step appears to necessitate translocation of the folded, metallated Rip1 across the IM. Bcs1 may mediate the extrusion of the Rip1 C-terminal globular domain with the Fe/S center across a bilayer. Mzm1 may stabilize a conformation of Rip1 that creates an optimal recognition interface for Bcs1. Studies are under way to assess whether Mzm1 mediates presentation of Rip1 to Bcs1.

ACKNOWLEDGMENTS

This work was supported by grant GM083292 to D.R.W. A.A. and P.S. were supported by training grant T32 DK007115. J.L.F. was supported by training grant T32 HL007576-25. O.K. was supported by American Heart Association fellowship 10POST4300044.

REFERENCES

1. **Atkinson, A., et al.** 2010. Mzm1 influences a labile pool of mitochondrial zinc important for respiratory function. J. Biol. Chem. **285:**19450–19459.

2. **Brandt, U., S. Uribe, H. Schagger, and B. L. Trumpower.** 1994. Isolation and characterization of *QCR10*, the nuclear gene encoding the 8.5-kDa subunit 10 of the *Saccharomyces cerevisiae* cytochrome bc_1 complex. J. Biol. Chem. **269:**12947–12953.
3. **Crivellone, M. D., M. A. Wu, and A. Tzagoloff.** 1988. Assembly of the mitochondrial membrane system. Analysis of structural mutants of the yeast coenzyme QH2-cytochrome *c* reductase complex. J. Biol. Chem. **263:**14323–14333.
4. **Cruciat, C. M., S. Brunner, F. Baumann, W. Neupert, and R. A. Stuart.** 2000. The cytochrome bc_1 and cytochrome *c* oxidase complexes associate to form a single supracomplex in yeast mitochondria. J. Biol. Chem. **275:**18093–18098.
5. **Cruciat, C. M., K. Hell, H. Folsch, W. Neupert, and R. A. Stuart.** 1999. Bcs1, an AAA-family member, is a chaperone for the assembly of the cytochrome bc_1 complex. EMBO J. **18:**5226–5233.
6. **Diekert, K., A. I. De Kroon, G. Kispal, and R. Lill.** 2001. Isolation and subfractionation of mitochondria from the yeast *Saccharomyces cerevisiae*. Methods Cell Biol. **65:**37–51.
7. **Edwards, C. A., and B. L. Trumpower.** 1986. Resolution and reconstitution of the iron-sulfur protein of the cytochrome bc_1 segment of the mitochondrial respiratory chain. Methods Enzymol. **126:**211–224.
8. **Esser, L., et al.** 2008. Inhibitor-complexed structures of the cytochrome bc_1 from the photosynthetic bacterium *Rhodobacter sphaeroides*. J. Biol. Chem. **283:**2846–2857.
9. **Ghezzi, D., et al.** 2011. Mutations in TTC19 cause mitochondrial complex III deficiency and neurological impairment in humans and flies. Nat. Genet. **43:**259–263.
10. **Ghezzi, D., et al.** 2011. SDHAF1, encoding a LYR complex-II specific assembly factor, is mutated in SDH-defective infantile leukoencephalopathy. Nat. Genet. **43:**259–265.
11. **Graham, L. A., U. Brandt, and B. L. Trumpower.** 1994. Protease maturation of the Rieske iron-sulphur protein after its insertion into the mitochondrial cytochrome bc_1 complex of *Saccharomyces cerevisiae*. Biochem. Soc. Trans. **22:**188–191.
12. **Graham, L. A., J. D. Phillips, and B. L. Trumpower.** 1992. Deletion of subunit 9 of the *Saccharomyces cerevisiae* cytochrome bc_1 complex specifically impairs electron transfer at the ubiquinol oxidase site (center P) in the bc_1 complex. FEBS Lett. **313:**251–254.
13. **Graham, L. A., and B. L. Trumpower.** 1991. Mutational analysis of the mitochondrial Rieske iron-sulfur protein of *Saccharomyces cerevisiae*. III. Import, protease processing, and assembly into the cytochrome bc_1 complex of iron-sulfur protein lacking the iron-sulfur cluster. J. Biol. Chem. **266:**22485–22492.
14. **Gruschke, S., et al.** 2011. Cbp3-Cbp6 interacts with the yeast mitochondrial ribosomal tunnel exit and promotes cytochrome *b* synthesis and assembly. J. Cell Biol. **193:**1101–1114.
15. **Hartl, F. U., B. Schmidt, E. Wachter, H. Weiss, and W. Neupert.** 1986. Transport into mitochondria and intramitochondrial sorting of the Fe/S protein of ubiquinol-cytochrome *c* reductase. Cell **47:**939–951.
16. **Heinemeyer, J., H. P. Braun, E. J. Boekema, and R. Kouril.** 2007. A structural model of the cytochrome *c* reductase/oxidase supercomplex from yeast mitochondria. J. Biol. Chem. **282:**12240–12248.
17. **Hu, J., L. Dong, and C. E. Outten.** 2008. The redox environment in the mitochondrial intermembrane space is maintained separately from the cytosol and matrix. J. Biol. Chem. **283:**29126–29134.
18. **Iwata, S., et al.** 1998. Complete structure of the 11-subunit bovine mitochondrial cytochrome bc_1 complex. Science **281:**64–71.
19. **Kronekova, Z., and G. Rodel.** 2005. Organization of assembly factors Cbp3 and Cbp4 and their effect on bc_1 complex assembly in *Saccharomyces cerevisiae*. Curr. Genet. **47:**203–212.
20. **Lange, H., A. Kaut, G. Kispal, and R. Lill.** 2000. A mitochondrial ferredoxin is essential for biogenesis of cellular iron-sulfur proteins. Proc. Natl. Acad. Sci. U. S. A. **97:**1050–1055.
21. **Lill, R., and U. Muhlenhoff.** 2008. Maturation of iron-sulfur proteins in eukaryotes: mechanisms, connected processes, and diseases. Annu. Rev. Biochem. **77:**669–700.
22. **Mathieu, L., S. Marsy, Y. Saint-Georges, C. Jacq, and G. Dujardin.** 2011. A transcriptome screen in yeast identifies a novel assembly factor for the mitochondrial complex III. Mitochondrion **11:**391–396.
23. **Merbitz-Zahradnik, T., K. Zwicker, J. H. Nett, T. A. Link, and B. L. Trumpower.** 2003. Elimination of the disulfide bridge in the Rieske iron-sulfur protein allows assembly of the [2Fe-2S] cluster into the Rieske protein but damages the ubiquinol oxidation site in the cytochrome bc_1 complex. Biochemistry **42:**13637–13645.
24. **Mumberg, D., R. Muller, and M. Funk.** 1994. Regulatable promoters of *Saccharomyces cerevisiae*: Comparison of transcriptional activity and their use of heterologous expression. Nucleic Acids Res. **22:**5767–5768.
25. **Nett, J. H., and B. L. Trumpower.** 1996. Dissociation of import of the Rieske iron-sulfur protein into *Saccharomyces cerevisiae* mitochondria from proteolytic processing of the presequence. J. Biol. Chem. **271:**26713–26716.
26. **Nett, J. H., and B. L. Trumpower.** 1999. Intermediate length Rieske iron-sulfur protein is present and functionally active in the cytochrome bc_1 complex of *Saccharomyces cerevisiae*. J. Biol. Chem. **274:**9253–9257.
27. **Nobrega, F. G., M. P. Nobrega, and A. Tzagoloff.** 1992. BCS1, a novel gene required for the expression of functional Rieske iron-sulfur protein in *Saccharomyces cerevisiae*. EMBO J. **11:**3821–3829.
28. **Phillips, J. D., L. A. Graham, and B. L. Trumpower.** 1993. Subunit 9 of the Saccharomyces cerevisiae cytochrome bc1 complex is required for insertion of EPR-detectable iron-sulfur cluster into the Rieske iron-sulfur protein. J. Biol. Chem. **268:**11727–11736.
29. **Pierrel, F., O. Khalimonchuk, P. A. Cobine, M. Bestwick, and D. R. Winge.** 2008. Coa2 is an assembly factor for yeast cytochrome *c* oxidase biogenesis facilitating the maturation of Cox1. Mol. Cell. Biol. **28:**4927–4939.
30. **Stuart, R. A.** 2008. Supercomplex organization of the oxidative phosphorylation enzymes in yeast mitochondria. J. Bioenerg. Biomembr. **40:**411–417.
31. **Vonck, J., and E. Schafer.** 2009. Supramolecular organization of protein complexes in the mitochondrial inner membrane. Biochim. Biophys. Acta **1793:**117–124.
32. **Wach, A., A. Brachat, C. Alberti-Segui, C. Rebischung, and P. Philippsen.** 1997. Heterologous *HIS3* marker and GFP reporter modules for PCR-targeting in *Saccharomyces cerevisiae*. Yeast **13:**1065–1075.
33. **Wiedemann, N., et al.** 2006. Essential role of Isd11 in mitochondrial iron-sulfur cluster synthesis on Isu scaffold proteins. EMBO J. **25:**184–195.
34. **Wittig, I., H. P. Braun, and H. Schagger.** 2006. Blue native PAGE. Nat. Protoc. **1:**418–428.
35. **Xia, D., et al.** 1997. Crystal structure of the cytochrome bc_1 complex from bovine heart mitochondria. Science **277:**60–66.
36. **Zara, V., L. Conte, and B. L. Trumpower.** 2009. Biogenesis of the yeast cytochrome bc_1 complex. Biochim. Biophys. Acta **1793:**89–96.
37. **Zara, V., L. Conte, and B. L. Trumpower.** 2009. Evidence that the assembly of the yeast cytochrome bc_1 complex involves the formation of a large core structure in the inner mitochondrial membrane. FEBS J. **276:**1900–1914.
38. **Zara, V., L. Conte, and B. L. Trumpower.** 2007. Identification and characterization of cytochrome bc_1 subcomplexes in mitochondria from yeast with single and double deletions of genes encoding cytochrome bc_1 subunits. FEBS J. **274:**4526–4539.
39. **Zollner, A., G. Rodel, and A. Haid.** 1994. Expression of the *Saccharomyces cerevisiae CYT2* gene, encoding cytochrome c_1 heme lyase. Curr. Genet. **25:**291–298.
40. **Zollner, A., G. Rodel, and A. Haid.** 1992. Molecular cloning and characterization of the *Saccharomyces cerevisiae CYT2* gene encoding cytochrome-c_1-heme lyase. Eur. J. Biochem. **207:**1093–1100.